

Electronic Supporting Information

High Surface Area and Z' in a Thermally Stable 8-Fold Polycatenated Hydrogen-Bonded Framework

Cassandra A. Zentner*, Holden W.H. Lai, Joshua T. Greenfield, Ren A. Wiscons, Matthias Zeller, Charles F. Campana, Orhan Talu, Stephen A. FitzGerald, Jesse L.C. Rowsell†

Table of Contents:

1. General Materials and Instrumentation	S-2
2. Synthesis	S-3
3. Crystallization Methods	S-4
Figure S1: Crystal habits for ethanol solvated tcpb	
4. Single Crystal Determination and Results	S-6
Table S1: Crystal data results	
5. Single Crystal Structure Details	S-9
Figure S2: Four possible conformations of tcpb	
Figure S3: Stacking representations of <i>I2</i> polymorph	
Figure S4: Stacking representation of <i>P1</i> polymorph	
Figure S5: π - π interactions at boundaries between 3 and 4 layered hexagonal sets	
Figure S6: Centroid to centroid distances in <i>I2</i> polymorph	
Figure S7: Centroid to centroid distances in <i>P1</i> polymorph	
Figure S8: Depiction of solvent accessible void volume	
6. Thermal Analysis Data	S-17
Figure S9: Calculated PXRD patterns	
Figure S10: PXRD comparison of ethanol and THF/H ₂ O solvated crystals	
Figure S11: ¹ H NMR of dried ethanol solvated crystals	
Figure S12: VT PXRD of THF/H ₂ O solvated crystals around the phase change	
Figure S13: VT PXRD of THF/H ₂ O solvated crystals, attempted THF/H ₂ O regeneration	
Figure S14: VT PXRD of THF/H ₂ O solvated crystals, ethanol regeneration	
Table S2: Unit cell parameters around the phase change	
Figure S15: Unit cell volume around the phase change	
7. Porosity Analysis	S-22
Figure S16: Nitrogen adsorption isotherms in tcpb	
Figure S17: BET plots with Rouquerol criteria	
Figure S18: Hydrogen adsorption isotherms in tcpb	
Table S3: Regression results for Virial isotherm for hydrogen adsorption	
Figure S19: Carbon dioxide adsorption isotherms in tcpb	
8. References	S-26

1. General Materials and Instrumentation

All materials were used as received. Aluminum chloride (99%) and tetrahydrofuran (unstabilized) were obtained from Alfa Aesar. 1,3,5-triphenylbenzene (97%), acetyl chloride, 1,4-dioxane (ACS grade), bromine, 1-propanol, 1-butanol and tetrahydrofuran (stabilized with butylated hydroxytoluene) were obtained from Sigma Aldrich. Dichloromethane, 2-propanol and absolute ethanol were obtained from Pharmco-Aaper. Magnesium sulfate (anhydrous), sodium bicarbonate, and sodium hydroxide pellets were obtained from J. T. Baker. Dimethylformamide- d_7 (DMF- d_7) and chloroform- d ($CDCl_3$) were obtained from Cambridge Isotope Laboratories.

Nuclear Magnetic Resonance (NMR)

A Varian 400 MHz NMR spectrometer was used for collecting 1H and ^{13}C NMR spectra. Default instrument parameters were used. Built in auto-lock and gradient shim routines were performed before spectrum collected. Chemical shifts were calibrated relative to the solvent peaks.

Fourier Transform Infrared Spectrometry (FTIR)

FTIR spectra were acquired using a ThermoMattson Satellite FTIR with an Attenuated Total Reflection (ATR) device attached. All spectra were taken between 600 and 4000 cm^{-1} with a resolution of 8.0 cm^{-1} , 32 scans were acquired per sample.

Thermal Gravimetric Analysis & Differential Scanning Calorimetry (TGA/DSC)

Thermal analysis was performed on a Mettler Toledo TGA/DSC 1 STAR[®] System. The TGA and DSC analyses were performed simultaneously. DSC was used to determine melting points. TGA/DSC conditions were as follows: N_2 gas, 30-600 $^{\circ}C$, ramp 5 $^{\circ}C/min$.

Powder X-Ray Diffraction (PXRD)

PXRD patterns were measured using a Rigaku Ultima IV diffractometer, powered to 40 kV/44 mA, using Cu K-alpha radiation ($\lambda = 1.5418 \text{ \AA}$). Parallel beam geometry was used for all samples. Variable temperature PXRD was performed in parallel beam geometry. Each pattern was taken between 2 and 35 2θ at a rate of 2 $2\theta/min$. The temperature was raised at 2 $^{\circ}C/min$ and held at a set point for 5 min before each pattern was acquired.

2. Synthesis:

Synthesis of 1,3,5-tris(4-acetylphenyl)benzene

The synthesis of 1,3,5-tris(4-acetylphenyl)benzene was adapted from a published method.^[1] In a 1-L round bottom flask, under a slow flow of nitrogen, AlCl_3 (33 g, 0.25 mol) was dissolved in 180 mL of acetyl chloride (2.5 mol) and chilled in an ice/water bath. In a 250-mL flask, 1,3,5-triphenylbenzene (10 g, 0.033 mol) was dissolved in 200 mL of dried dichloromethane (DCM) and also chilled in an ice/water bath. Once cold, the DCM solution was transferred to a chilled, N_2 purged dropping funnel and gradually added to the cold AlCl_3 /acetyl chloride solution. After addition of the first few drops the solution turned a deep red color. After the addition was complete, the mixture was stirred at room temperature for 2 hrs while a precipitate formed. The reaction mixture was then slowly poured into a 2-L Erlenmeyer flask containing 1800 mL of ice and stirred overnight, forming a light yellow slurry. The DCM phase was isolated using a separatory funnel. The water phase was then washed with DCM (3×200 mL). The DCM phases were combined, washed with 5% sodium bicarbonate (2×200 mL), then dried over MgSO_4 and filtered. The solution was evaporated, yielding a cream colored solid. The solid was then stirred with 1 L of boiling ethanol for 30 min and filtered while hot. The hot ethanol washing was repeated until the solvent was no longer discolored. The filter cake was dried overnight, yielding 9.2 g of a white solid (0.021 mol, 64%).

^1H NMR (CDCl_3 , 400 MHz): δ (ppm) 2.65 (s, 9H), 7.78 (t-d, 6H), 7.85 (s, 3H), 8.08 (t-d, 6H)

^{13}C NMR (CDCl_3 , 100 MHz): δ (ppm) 26.93, 126.33, 127.71, 129.29, 136.60, 141.79, 145.27, 197.81

IR (ATR): $\nu_{\text{C=O}}$ 1670 cm^{-1} (s), $\nu_{\text{C=C}}$ 1600 cm^{-1} (m), $\nu_{\text{C=C-H}}$ 3020 cm^{-1} (w)

MP (TGA/DSC): 256°C

Synthesis of 1,3,5-tris(4-carboxyphenyl)benzene

The synthesis of 1,3,5-tris(4-carboxyphenyl)benzene was adapted from a published method.^[1] 1,3,5-tris(4-acetylphenyl)benzene (13 g, 0.030 mol) was suspended in 600 mL of 1,4-dioxane in a 1-L round bottom flask. A solution of NaOH (42 g, 1.05 mol) dissolved in 290 mL of water was placed in a freezer ($\sim -10^\circ\text{C}$) for 1 hr. Bromine (19 mL) was added slowly to the cold solution, with stirring, yielding a deep yellow solution. The NaOBr solution was added slowly to the dioxane suspension, forming a yellow emulsion. The reaction mixture was stirred at 60°C for 2 hr, and then cooled to room temperature. The unreacted NaOBr was quenched by adding a 5% $\text{Na}_2\text{S}_2\text{O}_3$ solution (100 mL). The reaction mixture was then stirred for 10 min and acidified with concentrated HCl (~ 50 mL) to a pH < 2. The white suspension that formed was filtered, stirred into 500 mL of water, and filtered. This process was repeated two more times. The filter cake was dried under suction overnight. The still wet filter cake was dried further by stirring the solid into 200 mL of ethanol and then filtering. The filter cake was dried under vacuum at 90°C overnight, yielding a pale yellow solid (9.8 g, 0.022 mol, 75%).

^1H NMR (DMF-d_7 , 400 MHz): δ (ppm) 8.19 (m, 12H), 8.25 (s, 3H), 13.39 (s)

^{13}C NMR (DMF-d_7 , 100 MHz): δ (ppm) 126.20, 127.88, 130.40, 130.77, 141.61, 144.69, 167.63

IR (ATR): $\nu_{\text{C=O}}$ 1682 cm^{-1} (s), $\nu_{\text{C=C}}$ 1601 cm^{-1} (m), $\nu_{\text{O-H}}$ 2400-3200 cm^{-1} (m-b)

MP (TGA/DSC): 322°C

3. Crystallization Methods:

Single crystals for XRD grown from ethanol: 10 g of tcpb was boiled in 3L of ethanol in a flask. The solution was hot filtered and allowed to cool. Shortly after standing a precipitate formed and was filtered off. The remaining filtrate was allowed to cool completely to room temperature. The mother liquor was left to slowly evaporate to yield crystals suitable for single crystal, thermal and porosity analysis (Figure S1). Crystals were obtained as beveled prisms of elongated needles and thick plates.

Single crystals grown from 1-propanol and 2-propanol: 5 mg of tcpb were mixed with 1 mL solvent in a 2 mL vial with silicone lined caps. The vials were heated to 100°C for 3 hrs and then allowed to cool to room temperature. Closed vials were left at room temperature and crystals formed after 5 days. Crystals were obtained as beveled prisms of elongated needles and thick plates.

Single crystals grown from 1-butanol: 10 mg of tcpb were mixed with 1 mL solvent in a 2 mL vial with silicone lined caps. The vial was heated to 120°C for 90 min and then allowed to cool to room temperature. Closed vials were left at room temperature and crystals formed after 5 days. Crystals were obtained as beveled prisms of elongated needles and thick plates.

Bulk crystallization from THF/H₂O: Recrystallized from 1 tetrahydrofuran (THF): 1 H₂O (v/v). For batch recrystallization, 5 g tcpb was transferred into a 1 L flask followed by addition of 250 mL of water and 250 mL of THF (both unstabilized and stabilized THF can be used). The flask was capped with a teflon-lined cap and shaken several times before it was placed in a 70°C oven for 4 hrs. During the first 2 hrs of heating, the flask was shaken every 30 min and was left undisturbed for the remaining 2 hrs in the oven, allowing the solvent mixture to fully phase separate. The flask was removed after 4 hrs of heating and placed on a benchtop to cool to room temperature. After cooling to room temperature, both phases were transparent. The bottle was briefly shaken to combine the two phases and immediately transferred to a 4°C refrigerator to promote crystal growth. After 10 days in the refrigerator with occasional shaking, the crystals were filtered, washed with ethanol, ether, and dried under vacuum. Crystals were obtained as beveled prisms of elongated needles and thick plates.

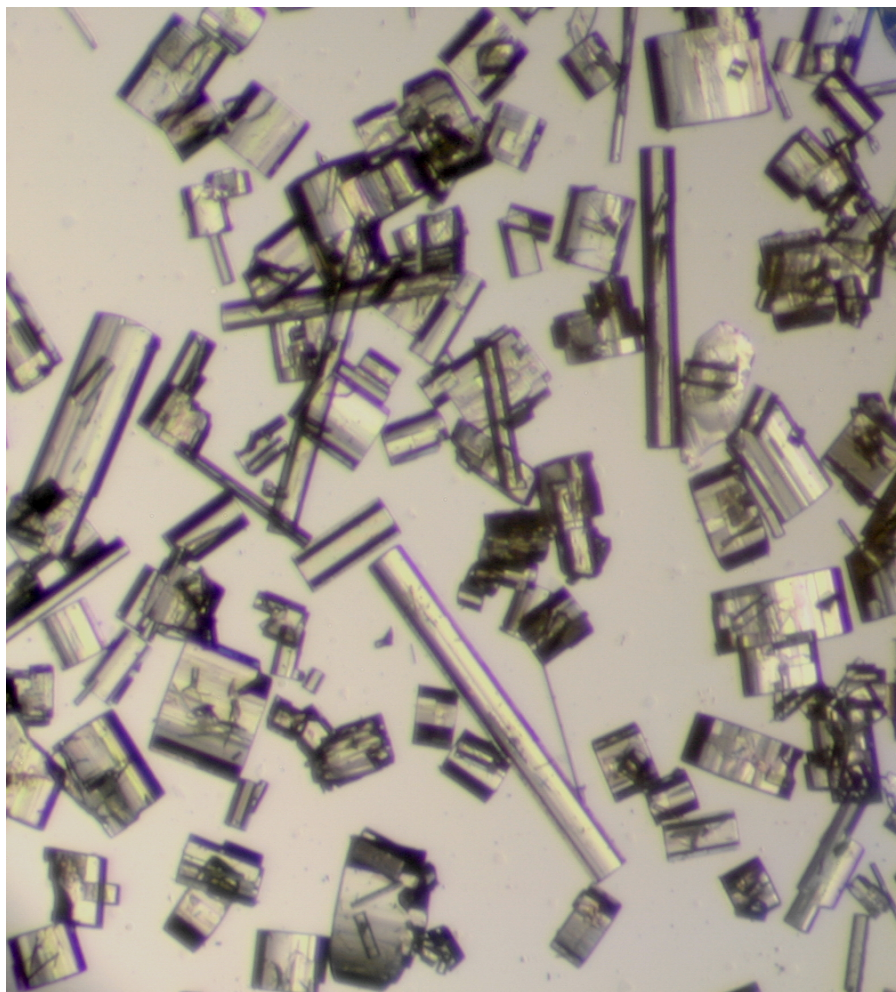


Figure S1: Crystal habits for ethanol solvated tcpb.

4. Single Crystal Determination and Results

Single crystal data were collected at the applications lab of Bruker AXS Inc in Madison, WI. Single crystals of 1,3,5-tris(4-carboxyphenyl)benzene were mounted on Mitegen micromesh mounts with the help of a trace of oil. Data of several crystals of both the *P1* and *I2* polymorphs from all tested solvents were collected which gave similar results.¹ Details are given for the best data set of each type (both grown from ethanol). Data for the *P1* structure were collected on a Bruker AXS X8 Prospector CCD diffractometer equipped with a copper I- μ -S microsource X-ray tube ($\lambda = 1.54178 \text{ \AA}$) and a laterally graded multilayer (Goebel) mirror for monochromatization. Data for the *I2* structure were collected on a Bruker AXS APEXII CCD diffractometer with a molybdenum sealed tube X-ray source ($\lambda = 0.71073 \text{ \AA}$) and Triumph curved graphite monochromator. Both instruments featured ApexII CCD area detectors. The Apex2 software package was used to determine unit cells and for data collection and data were integrated using SAINT V7.68A.^{2, 3} The data were processed with SADABS and corrected for absorption using multi-scan techniques.⁴

The space groups were assigned as *P1* and *I2* using XPREP of the Bruker SHELXTL package, solved with ShelXD, and refined with SHELXL 2014/7 and the graphical interface Shelxle.⁵⁻⁸ All non-hydrogen atoms were refined anisotropically. H atoms attached to carbon and hydroxyl oxygen atoms were positioned geometrically and constrained to ride on their parent atoms, with carbon hydrogen bond distances of 0.95 \AA for aromatic C-H and 0.84 \AA for carboxylic acid moieties, respectively. Hydroxyl H atoms were allowed to rotate but not to tip to best fit the experimental electron density, but were restrained to lie in a common plane with the C and O atoms of the carboxylic acid atoms. $U_{\text{iso}}(\text{H})$ values were set to a multiple of $U_{\text{eq}}(\text{C/O})$ with 1.5 for O-H and 1.2 for C-H, respectively. Both structures feature large solvent accessible volumes within the rigid framework of 1,3,5-tris(4-carboxyphenyl)benzene molecules. The contents of these volumes are highly disordered and the residual electron density peaks are not arranged in an interpretable pattern. The cif and fcf files were thus corrected for using reverse Fourier transform methods using the SQUEEZE routine as implemented in the program Platon (Version 191114, Feb 10, 2015).⁹ The resultant files were used in the further refinement. (The FAB files with details of the Squeeze results are appended to the cif files). The *P1* structure has a solvent accessible volume of 15672.6 \AA^3 . The Squeeze procedure corrected for 4462.9 electrons within the solvent accessible voids. The *I2* structure has a solvent accessible volume of 16285.9 \AA^3 . The Squeeze procedure corrected for 2063.7 electrons within the solvent accessible voids. Additional details are presented in Table 1 and are given as Supporting Information in a CIF file. Complete crystallographic data, in CIF format, have been deposited with the Cambridge Crystallographic Data Centre. CCDC 1400565-1400566 contains the supplementary crystallographic data for this paper. These data can be obtained free of charge from The Cambridge Crystallographic Data Centre via www.ccdc.cam.ac.uk/data_request/cif.

¹ An additional polymorph, similar to the *I2* and *P1* forms described but with half the unit cell volume, had been found in small amounts in some of the crystallization setups, but these could not be reproducibly formed and the quality of the crystals did not allow for a complete unambiguous single crystal structure refinement.

Table S1. Crystal data results

	From I	Form II
Crystal data		
Chemical formula	$C_{27}H_{18}O_6 \times \text{Solv}$	$C_{27}H_{18}O_6 \times \text{Solv}$
M_r	438.41	438.41
Crystal system, space group	Monoclinic, $I2$	Triclinic, $P1$
Temperature (K)	100	100
a, b, c (Å)	31.419 (6), 30.116 (6), 45.320 (9)	31.1904 (16), 31.2132 (14), 51.976 (3)
β (°)	90.412 (2)	72.710 (4), 77.555 (3), 60.912 (3)
V (Å ³)	42880 (14)	42068 (4)
Z, Z'	56, 14	56, 56
$F(000)$	12768	12768
Radiation type	Mo $K\alpha$	Cu $K\alpha$
μ (mm ⁻¹)	0.07	0.57
Crystal shape	Needle	Plate
Colour	Colourless	Colourless
Crystal size (mm)	$1.19 \times 0.24 \times 0.06$	$0.62 \times 0.15 \times 0.08$
Data collection		
Diffractometer	fixed-chi duo Bruker AXS APEXII CCD diffractometer	Bruker AXS Prospector CCD diffractometer
Radiation source	sealed X-ray tube	I- μ -S microsource X-ray tube
Monochromator	Triumph curved graphite monochromator	Laterally graded multilayer (Goebel) mirror
Scan method	ω and phi scans	ω and phi scans
Absorption correction	Multi-scan <i>SADABS</i> (Sheldrick, 2011)	Analytical <i>SADABS</i> (Sheldrick, 2011)
T_{\min}, T_{\max}	0.6747, 0.746	0.671, 0.745
No. of measured, independent and observed [$I > 2\sigma(I)$] reflections	246,101, 96,106, 46,684	148,299, 148,299, 73,443
R_{int}	0.060	---
θ values (°)	$\theta_{\max} = 27.5, \theta_{\min} = 1.8$	$\theta_{\max} = 68.4, \theta_{\min} = 1.6$
$(\sin \theta/\lambda)_{\max}$ (Å ⁻¹)	0.650	0.603
Range of h, k, l	$h = -40 \rightarrow 40, k = -39 \rightarrow 39, l = -58 \rightarrow 58$	$h = -34 \rightarrow 34, k = -31 \rightarrow 37, l = -31 \rightarrow 62$

Refinement		
$R[F^2 > 2\sigma(F^2)]$, $wR(F^2)$, S	0.053, 0.138, 0.90	0.069, 0.177, 0.89
No. of reflections	96,106	148,299
No. of parameters	4,201	16,805
No. of restraints	43	172
H-atom treatment	H-atom parameters constrained	H-atom parameters constrained
$(\Delta/\sigma)_{\max}$	0.006	0.001
$\Delta\rho_{\max}$, $\Delta\rho_{\min}$ (e Å ⁻³)	0.24, -0.25	0.44, -0.34
Extinction method	---	<i>SHELXL2014/7</i> (Sheldrick, 2014), $F_c^* = kF_c[1 + 0.001 \times F_c^2 \lambda^3 / \sin(2\theta)]^{-1/4}$
Extinction coefficient	---	0.000036 (3)
Absolute structure	Flack x determined using 16234 quotients [(I+)-(I-)]/[(I+)+(I-)] (Parsons, Flack and Wagner, Acta Cryst. B69 (2013) 249-259).	No quotients, so Flack parameter determined by classical intensity fit
Absolute structure parameter	0.4 (5)	-0.09 (7)

5. Crystal Structure Details

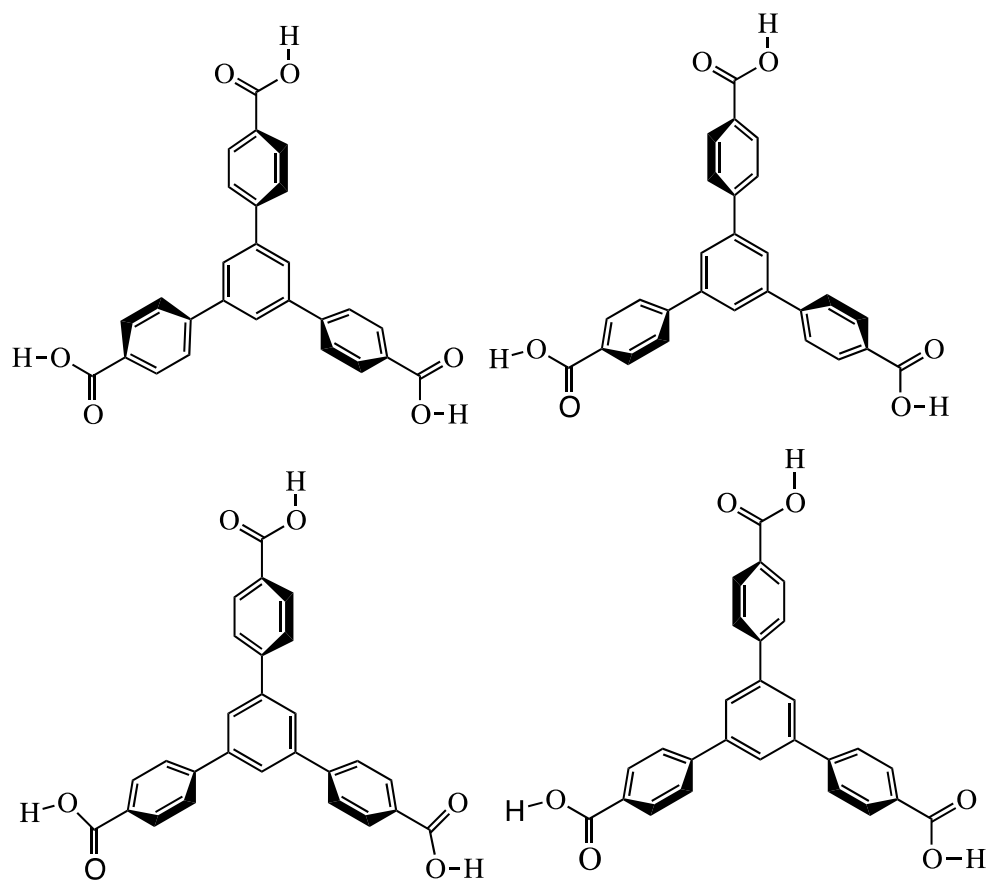
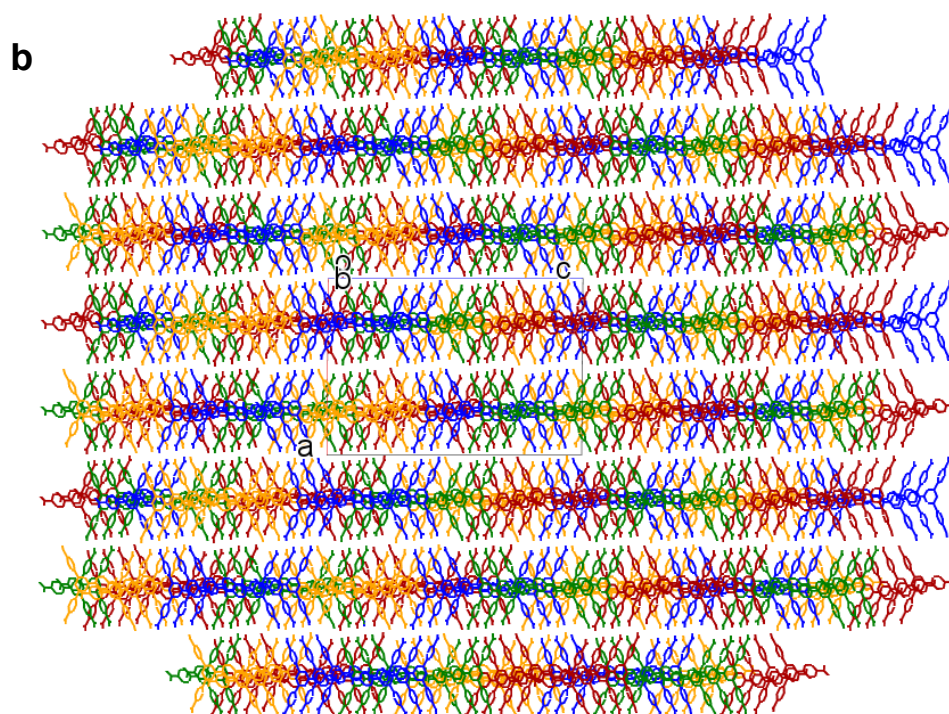
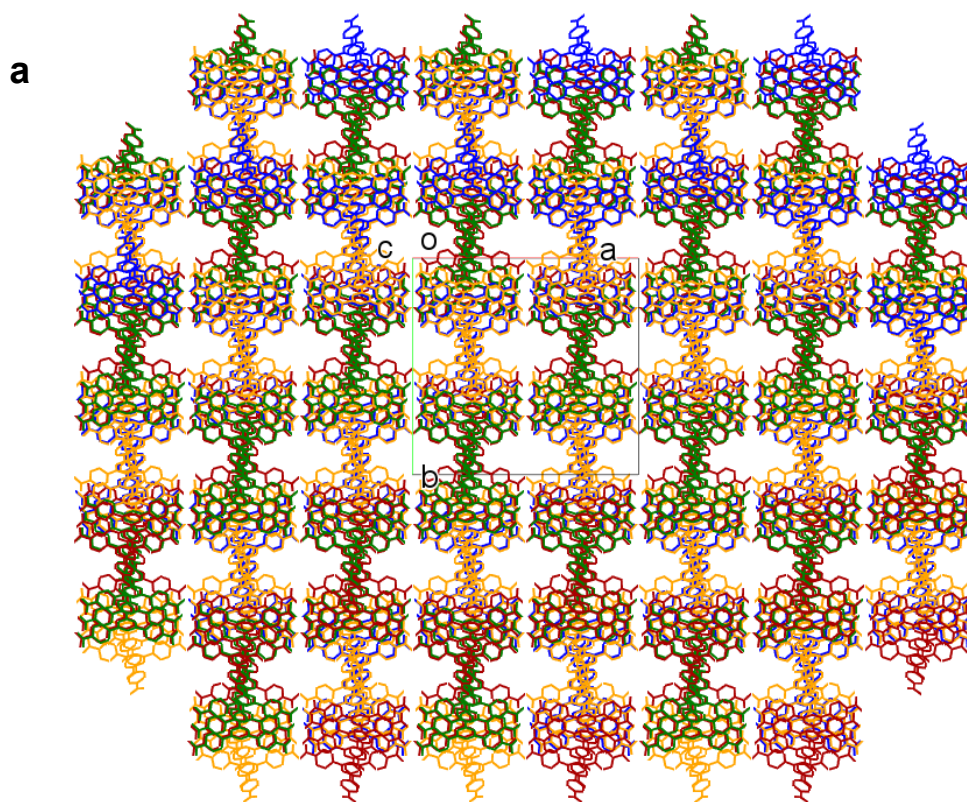


Figure S2: Four possible conformations of tcpb. The top two conformations are described as propellers (clockwise and counterclockwise), while the bottom are defect propellers (one blade oriented differently compared to clockwise or counterclockwise conformation above).



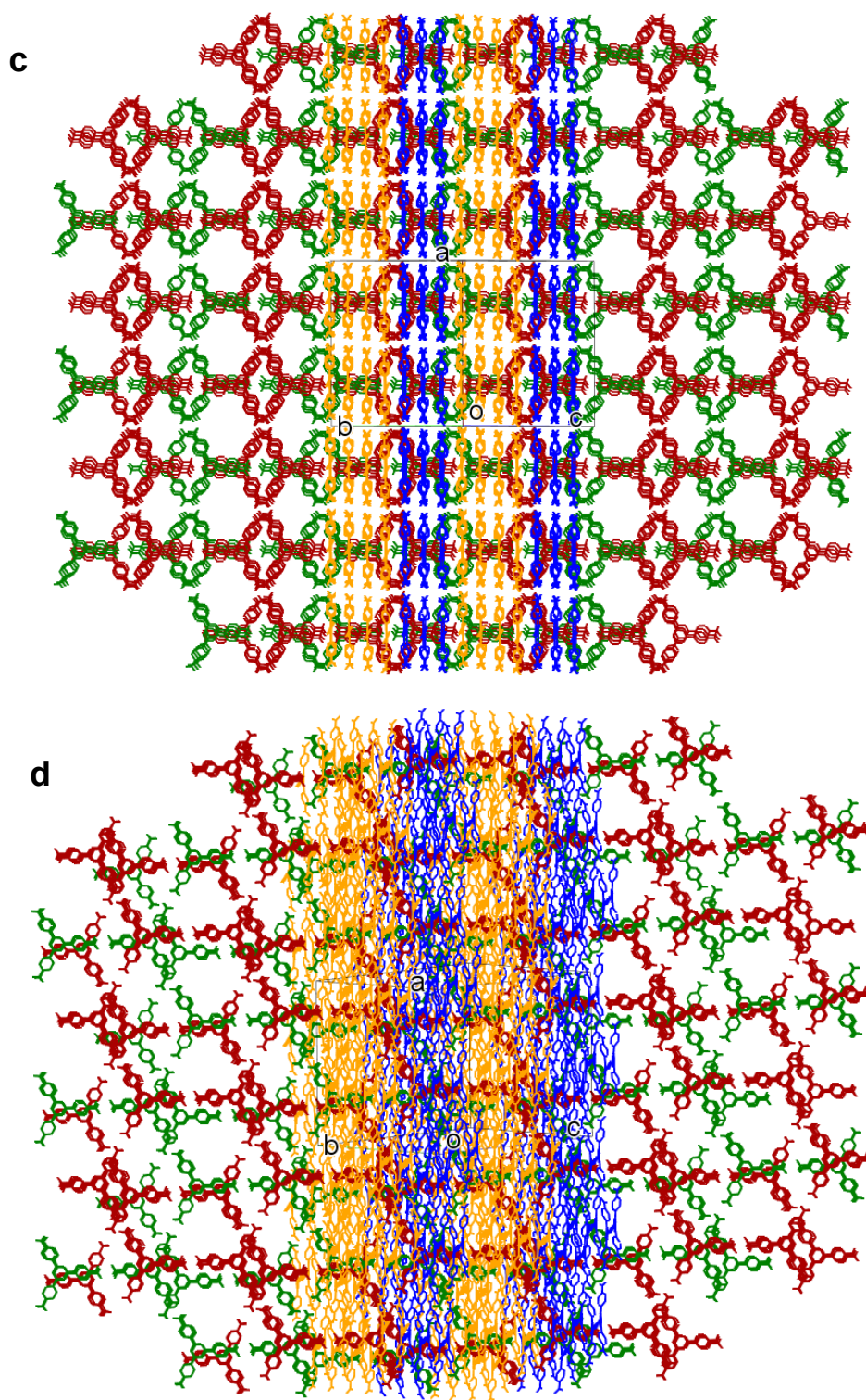
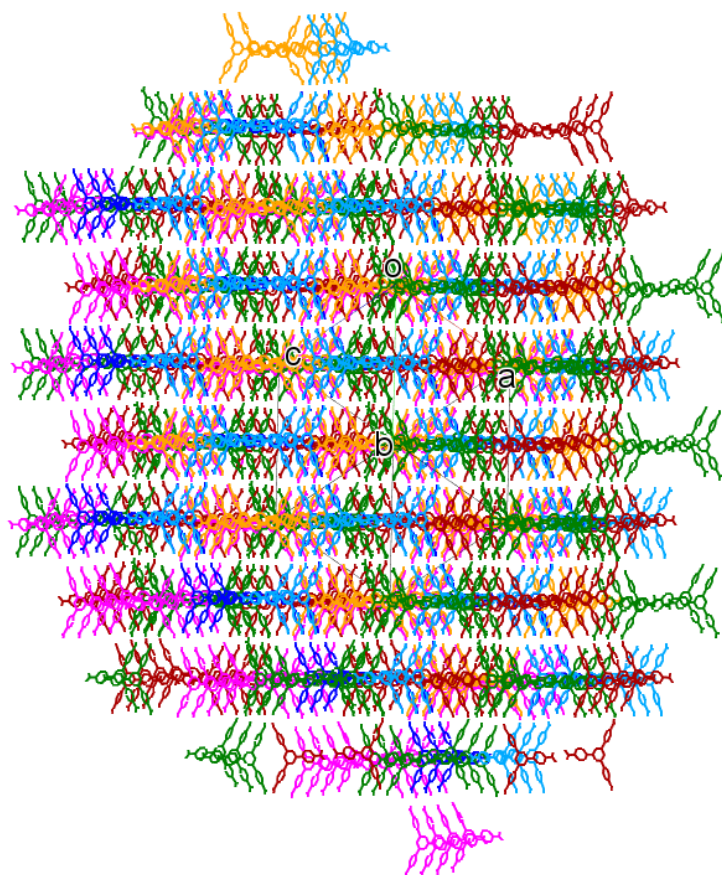
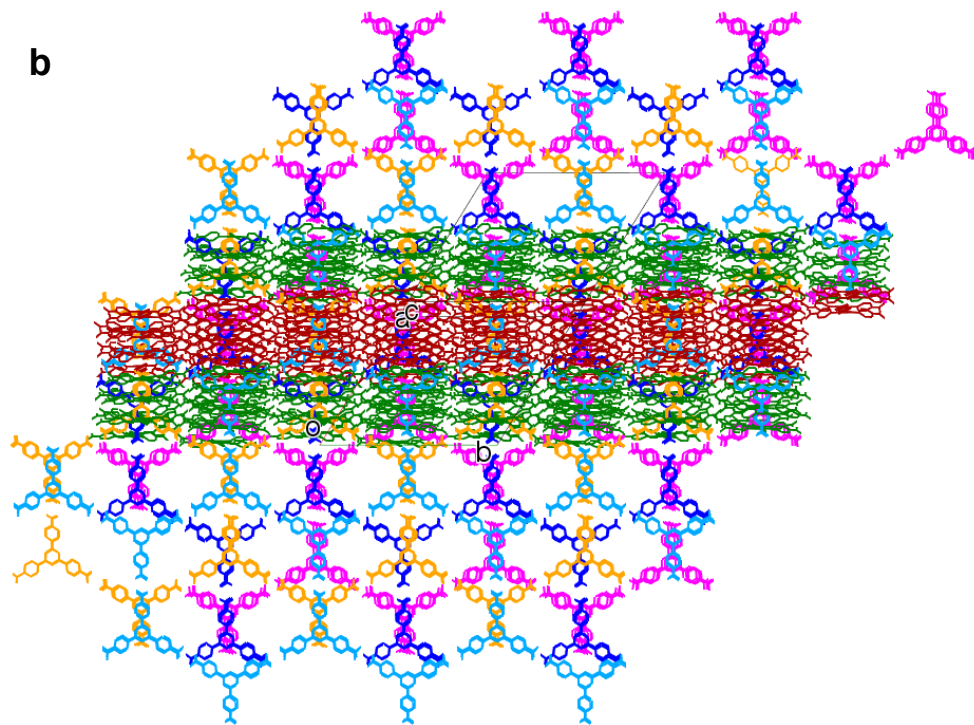


Figure S3: Representation of the stacking in the *I*₂ polymorph. Four stacks in red and yellow, three stacks in green and blue. Four and three stacks in the intercalated sheets are symmetry equivalent, related by two fold axis. View down the following: (a) (001); (b) (010); (c) (011); (d) slightly offset from (011)

a



b



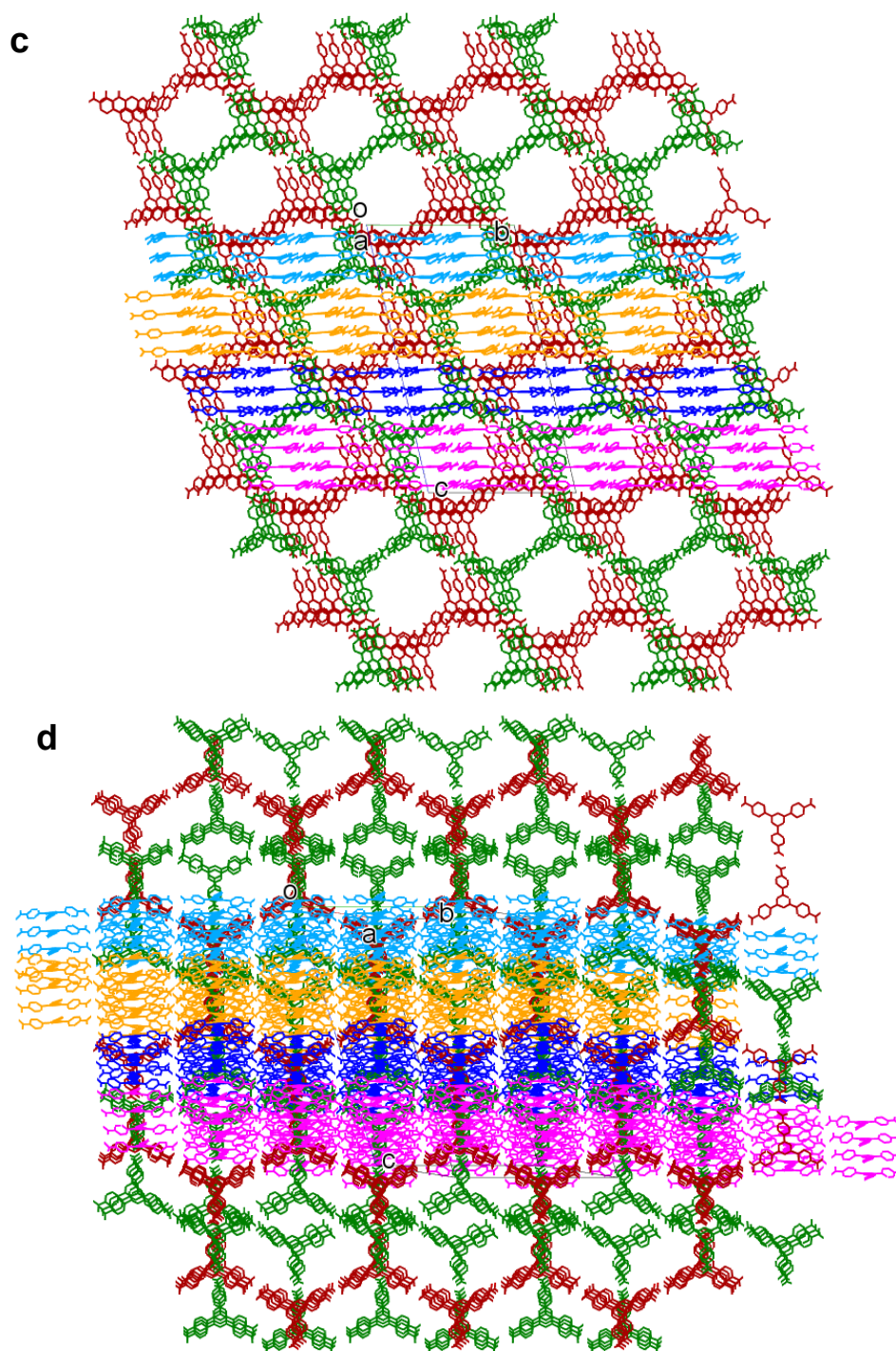


Figure S4: Representation of the stacking in the *P1* polymorph. 3 and 4 stacks along the *a*-axis (green and red, respectively) are related by simple translation. Stacks along the *c*-axis direction (light blue, yellow, blue and pink) are distinct and symmetry independent of each other. View down the follow: (a) (111); (b) (101); (c) (100); (d) reciprocal (100)

The differences between *I2* and *P1* polymorphs are illustrated by the centroid to centroid distances of the central benzene rings at the boundary between 3 and 4 layered stacks.

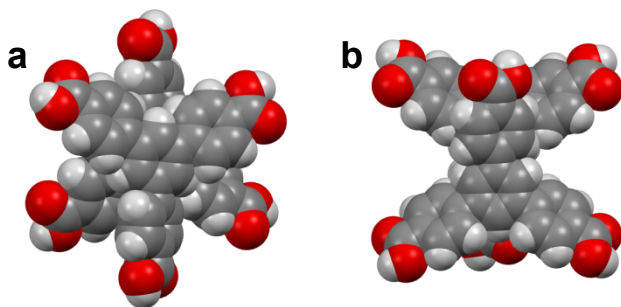


Figure S5: π - π interactions at boundaries between 3 and 4 layered hexagonal sets. (a) First interaction where the central benzene rings of both molecules are directly on top of each other; (b) interaction where the central benzene ring interacts with the phenyl ring of the other molecule.

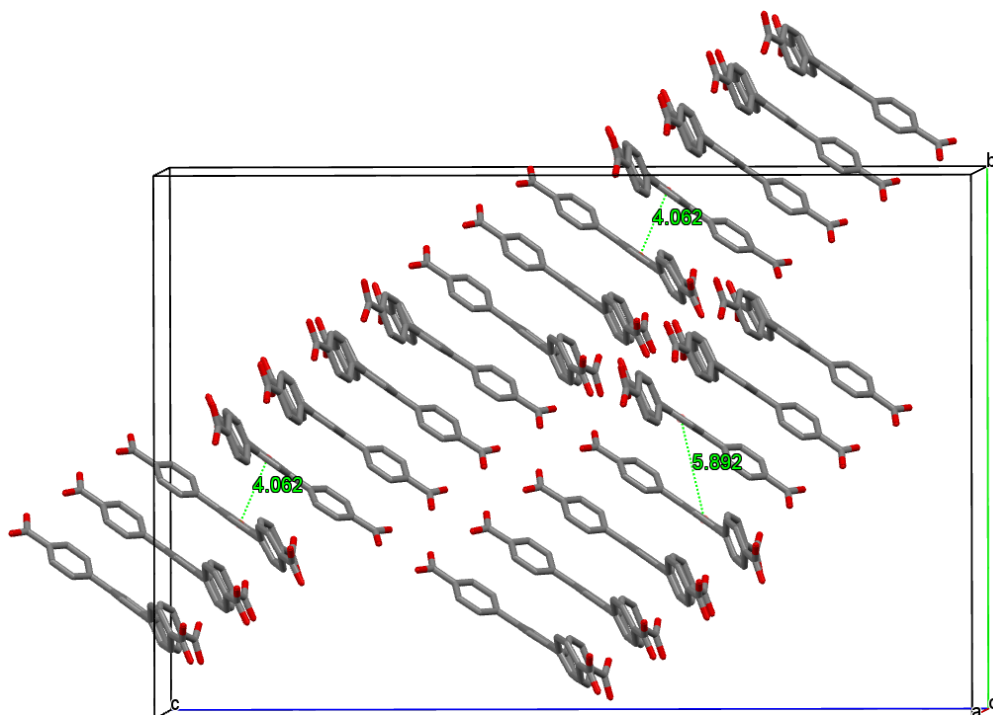


Figure S6: Centroid to centroid distances in the *I2* polymorph. Red spheres represent benzene ring centroids, and dashed green lines show centroid to centroid distances. Two distances are observed: 4.062 Å and 5.892 Å. The two alternating centroid to centroid distances match with the observed ABAB stacking of layers.

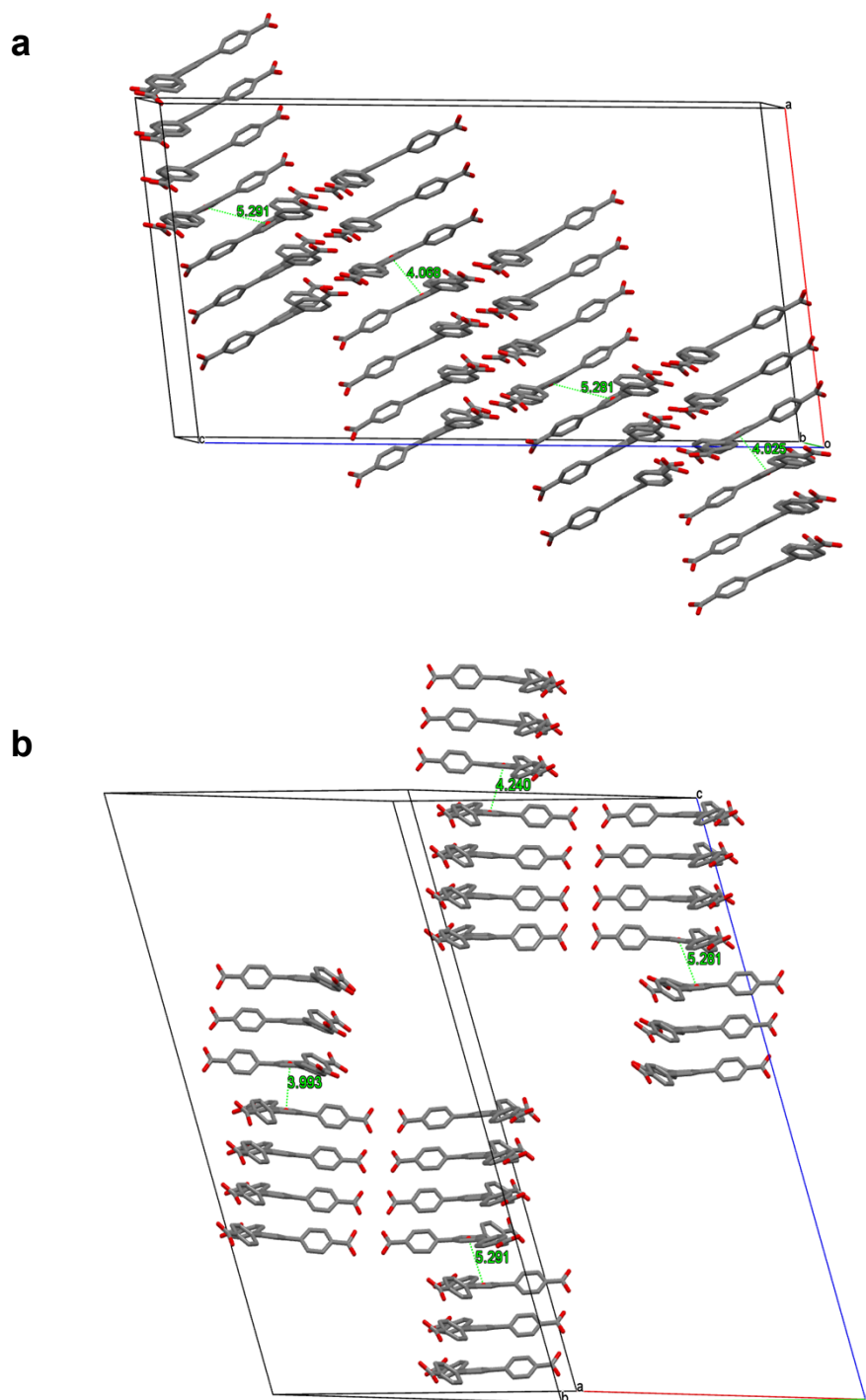


Figure S7: Centroid to centroid distances in *P1* polymorph (a) ABABAB symmetry layer; (b) ABA'B' symmetry layer. Red spheres represent benzene ring centroids, and dashed green lines show centroid to centroid distances. In the *P1* polymorph six interactions are present with central benzene centroid to centroid distances of 4.025, 3.993, 4.240, 4.068, 5.291 and 5.281 Å. The six observed centroid to centroid distances match the three sets of crystallographically independent 3 plus 4 stacks of hexagonal sheets.

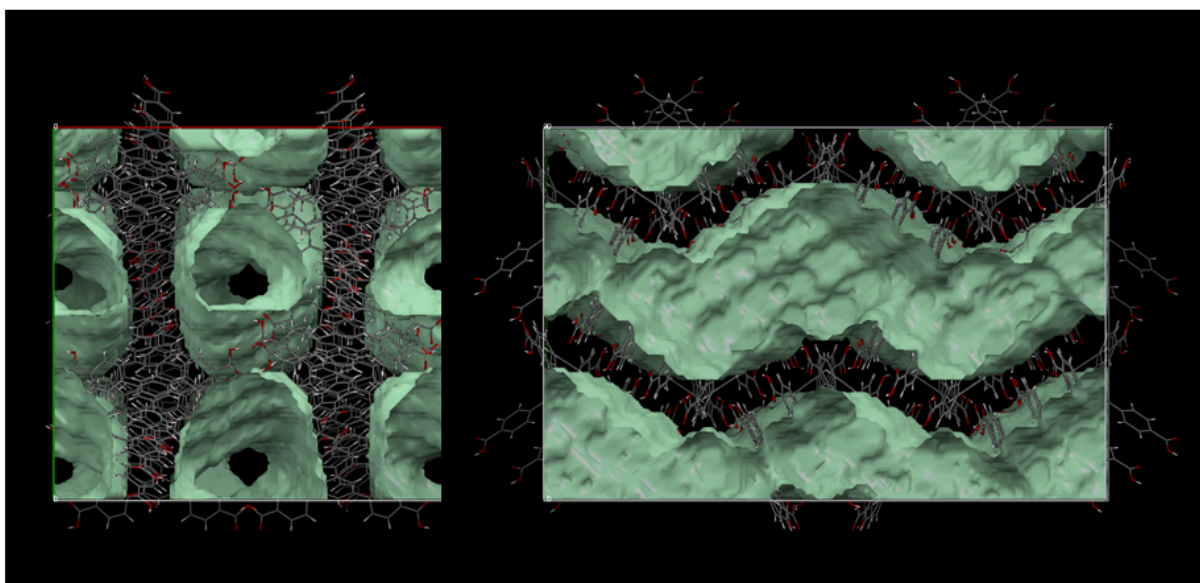


Figure S8: Depiction of solvent accessible void volume. Shown is the *I2* polymorph. Approximately 38% of the crystal volume forms continuous channels.

6. Thermal Analysis Data

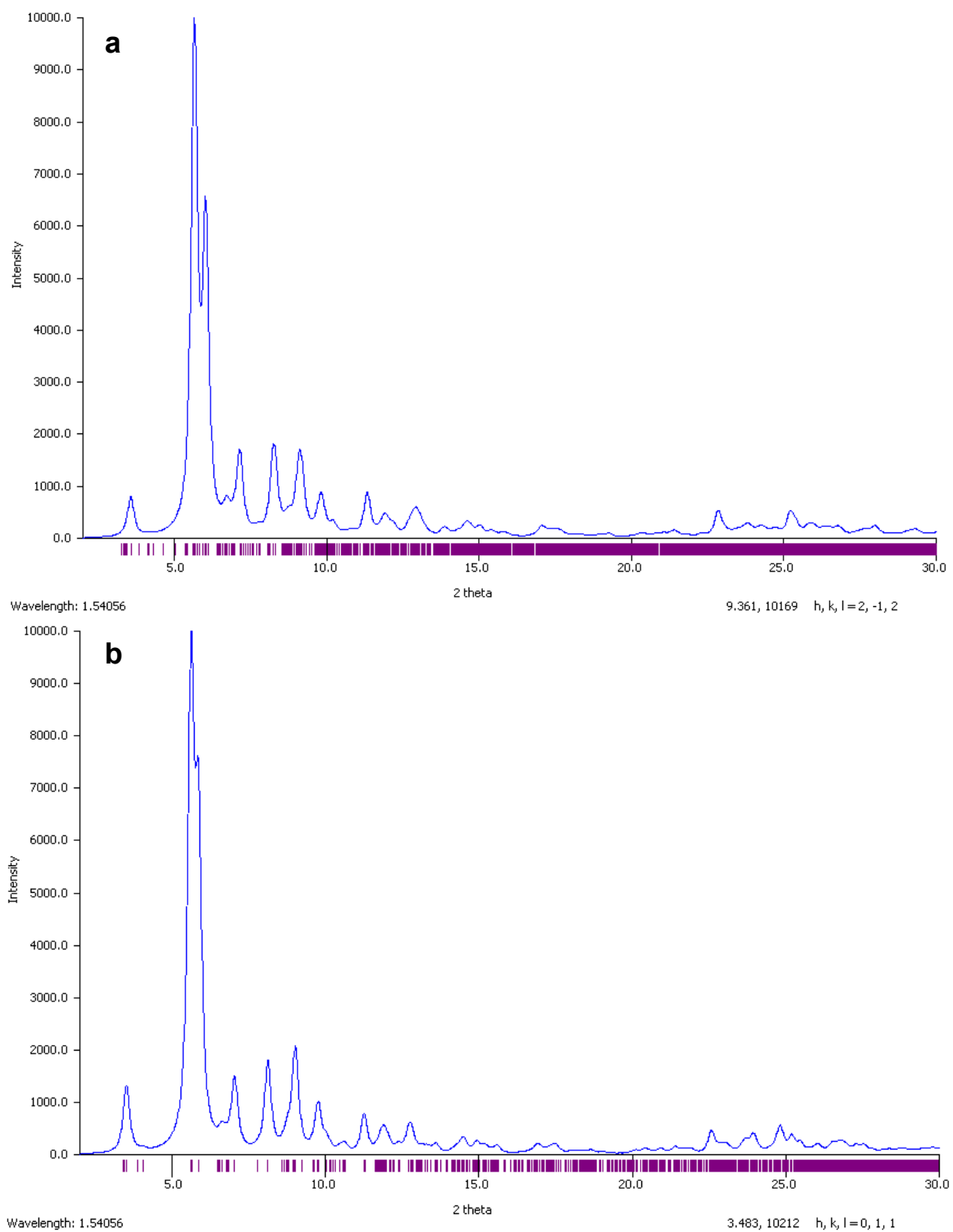


Figure S9: Calculated PXRD patterns, simulated from the single crystal data (after correction by Squeeze). (a) *P1* structure; (b) *I2* structure

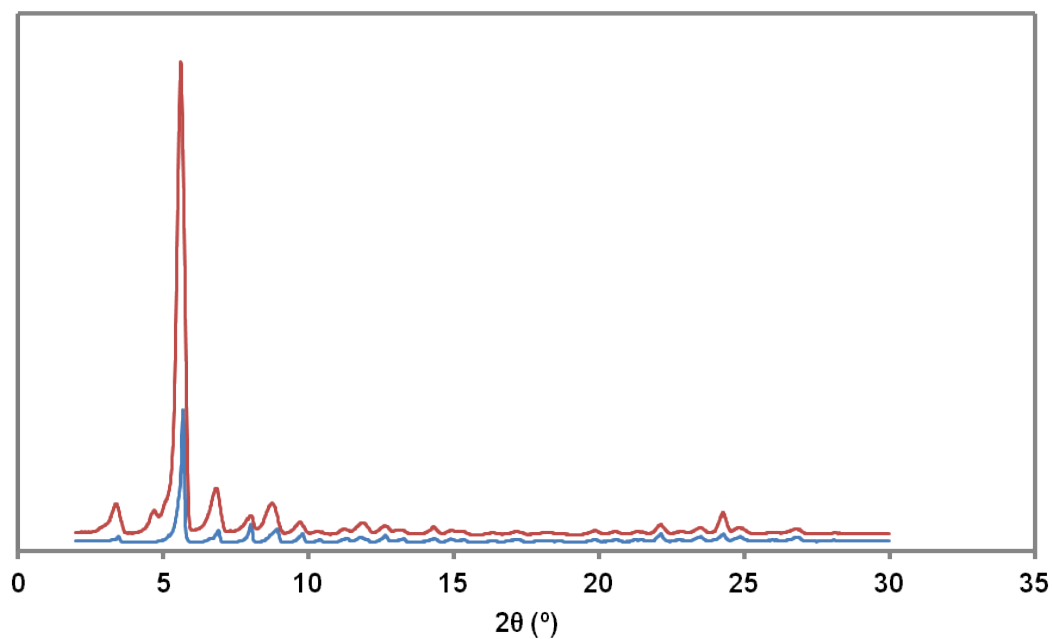


Figure S10: PXRD comparison of ethanol (blue) and THF/H₂O (red) solvated crystals, measurements taken at 90°C under N₂.

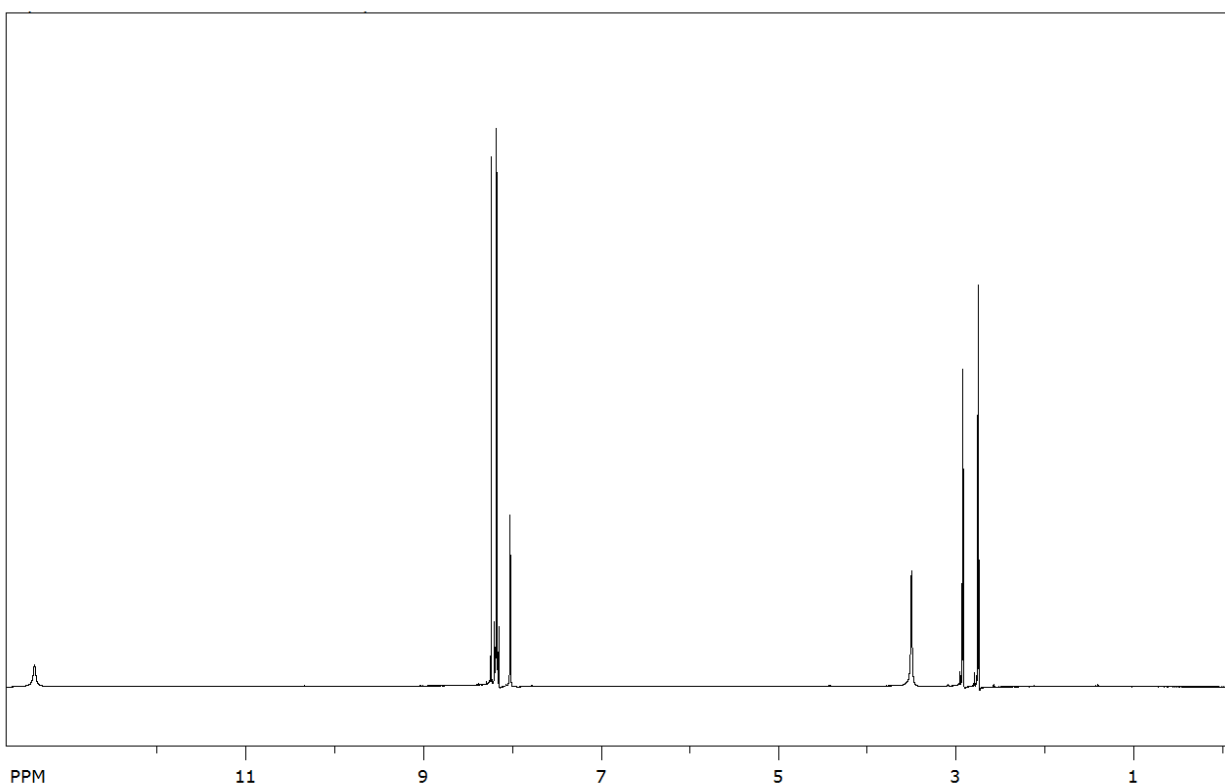


Figure S11: ¹H NMR of dried ethanol solvated crystals, in DMF-d₇. The crystals were dried using the TGA, by heating at 5°C/min to 130°C, and dried for 4 hrs. No solvent present after heating to 130°C. DMF-d₇ solvent peaks at 2.74, 2.92, and 8.03 ppm. Water impurity is present in the DMF-d₇ at 3.50 ppm.

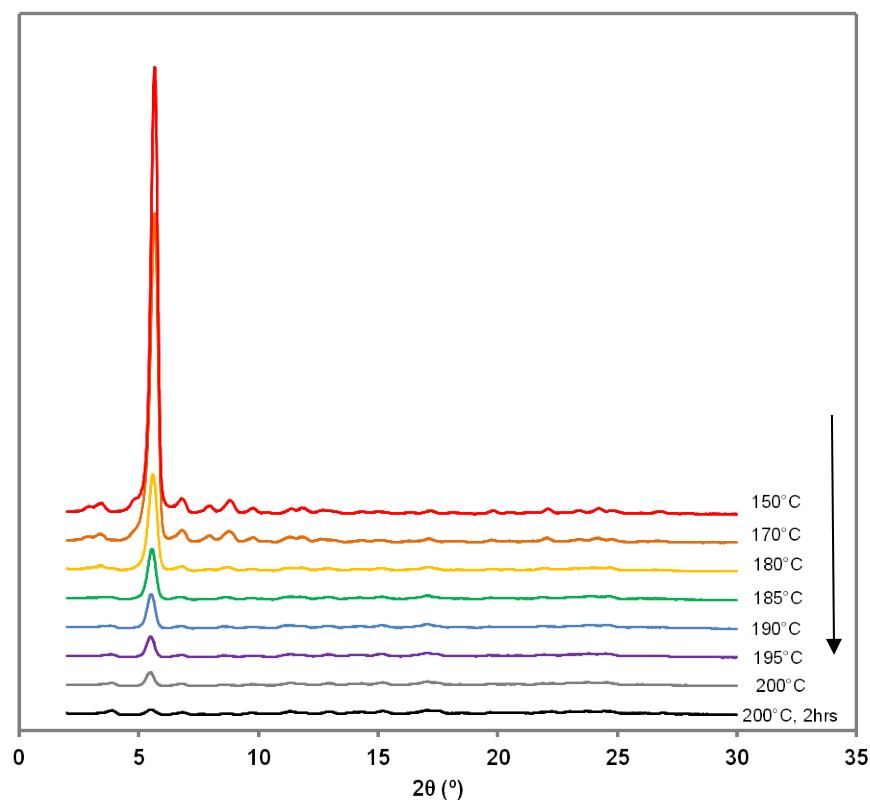


Figure S12: VT PXRD of THF/H₂O solvated crystals around the phase change, measured under N₂. Arrow indicates sequence of patterns taken.

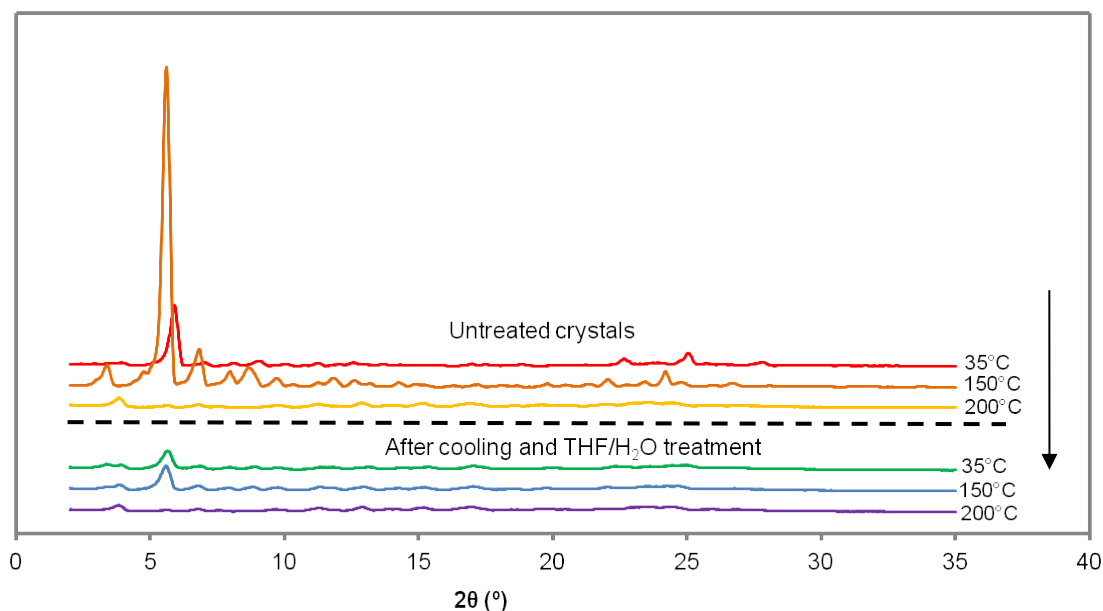


Figure S13: VT PXRD analysis of THF/H₂O solvated crystals, attempted THF/H₂O regeneration, measured under N₂. After patterns were taken up to 200°C, the crystals were cooled down to room temperature. The crystals were soaked in THF/H₂O (1:1) to attempt regeneration and the VT PXRD experiment was repeated. The attempted regeneration with the recrystallization solvent did not fully regenerate the structure, unlike the ethanol treatment of the ethanol solvated crystals. Arrow indicates sequence of patterns taken.

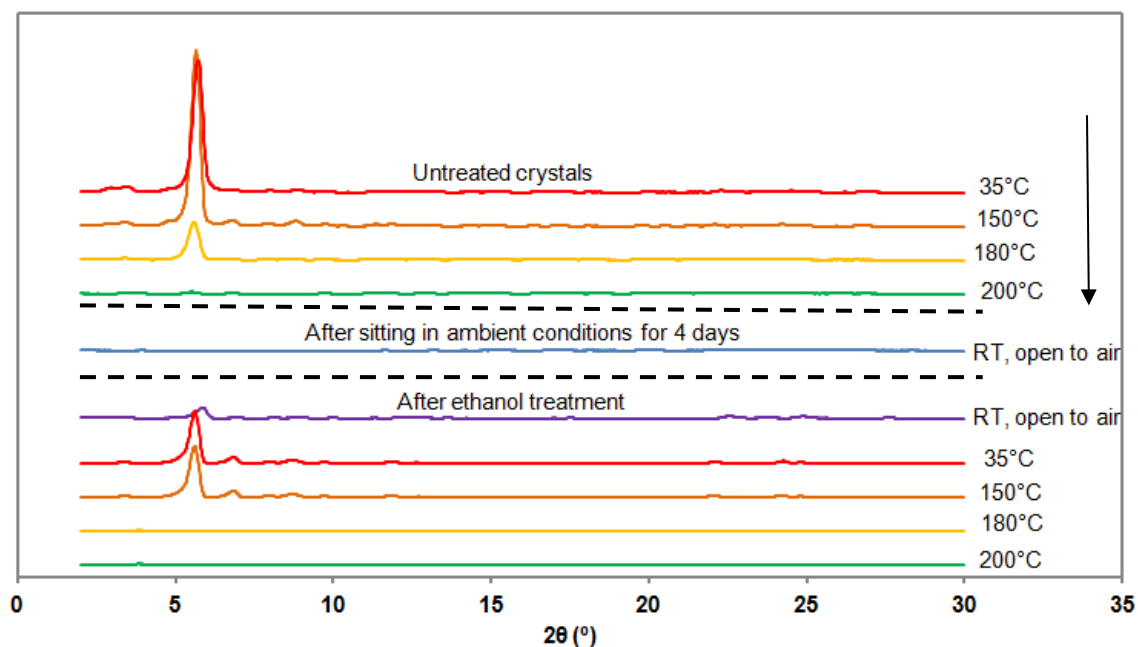


Figure S14: VT PXRD analysis of THF/H₂O solvated crystals, before and after ethanol treatment, measured under N₂, unless otherwise indicated. After cooling from 200°C, the crystals were left in ambient conditions for 4 days. The PXRD pattern was not regenerated. Crystals were then soaked in ethanol overnight, filtered, and the VT PXRD experiment was repeated. The PXRD pattern and crystal structure were regenerated. The structure of the ethanol treated crystals collapsed by 180°C, unlike the 200°C before treatment. Arrow indicates the sequence of the patterns taken.

	a (Å)	b (Å)	c (Å)	α (°)	β (°)	γ (°)	Vol (Å ³)
100 K	29.7437	31.3442	31.3089	119.6172	118.0608	90.3459	21282.648
300 K	30.3972	31.0642	31.3253	119.4582	118.6735	90.3033	21440.324
350 K	30.6659	31.0850	31.3964	119.3588	118.8788	90.3181	21658.822
400 K	31.0073	31.0873	31.4506	119.3582	119.2257	90.3366	21827.733
430 K	30.9507	31.0380	31.5179	119.2822	119.3842	90.0916	21817.688
440 K	31.0270	31.0735	31.4576	119.4038	119.1319	90.1635	21882.870
450 K	31.0597	31.1008	31.5477	119.1763	119.5434	90.0270	21954.042
460 K	31.0270	31.0735	31.4576	119.4038	119.1319	90.1635	21882.870
470 K	26.9347	31.1281	31.2454	119.0976	114.2525	91.0450	20074.002
480 K	26.0431	31.2329	31.6638	119.9592	113.1331	90.3989	19841.534

Table S2: Unit cell parameters around the phase change. Data were obtained from single crystal diffraction on a Bruker CMOS diffractometer equipped with an Oxford cryosystems 700Plus variable temperature device. A crystal of the *I*2 type was mounted at room temperature with high boiling high viscosity oil and cooled at a rate of 360°C/hr to 100 K. Unit cell data were obtained upon rewarming at the same rate, with the crystal being allowed to equilibrate for 10 min at each temperature. Crystals maintain their shape and remain single up to a temperature of 460 K (187 °C). Upon further heating, crystals break up into multiple smaller pieces, but individual pieces remained large enough for determination of unit cell parameters. Unit cell parameters are given for the reduced primitive cell for easier comparison of values before and after phase change (which is accompanied by loss of the I-centered monoclinic symmetry).

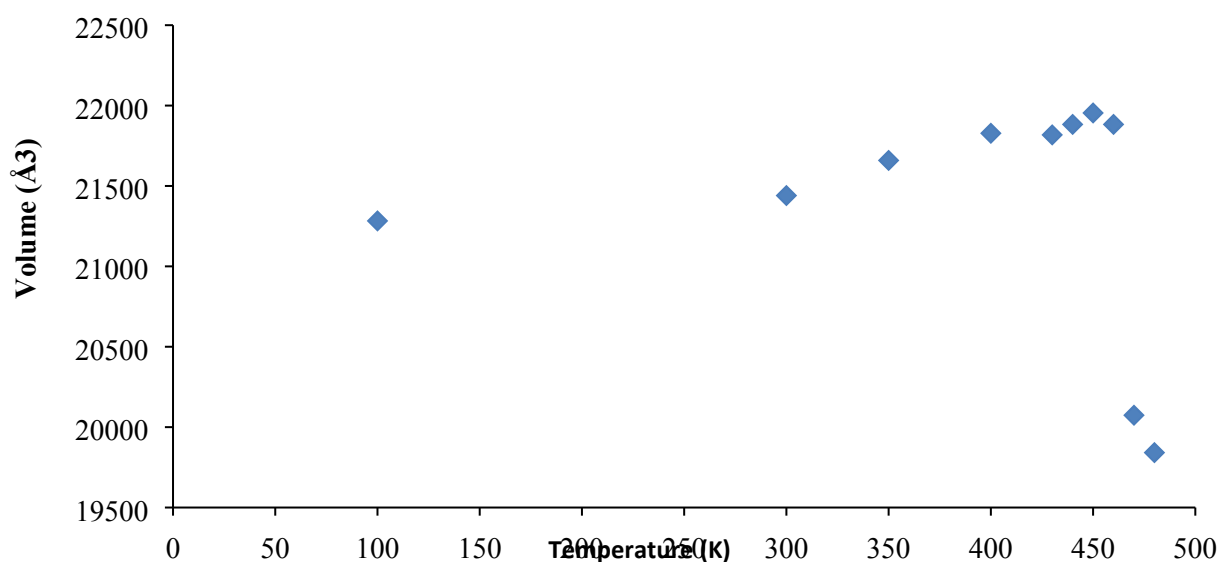


Figure S15: Unit cell volume around the phase change.

7. Porosity Analysis

Three sets of adsorption experiments were performed: 1) nitrogen adsorption at 77.35 K to determine BET surface area, pore size, and volume, 2) hydrogen isotherms at 77.35 and 87.15 K, and 3) carbon dioxide isotherms around RT, to determine isotherms and isosteric heat of adsorption. A Micromeritics ASAP 2010 apparatus was used. The samples were completely outgassed at 130°C assured by stable pressure in sample cell of less than 70 microtorr for over a 30 min period. Initial activation took over 16 hrs, subsequent activations were complete within 2-3 hrs. The samples were heated slowly (i.e. 1°C/min.) during activation. The initial weight loss of the samples was in agreement with solvent amount in the porous space within the accuracy of external weight measurements under helium atmosphere. Cold and room temperature dead volume in the sample tubes were measured with helium, thus results are examined within the helium-surface excess amount adsorbed thermodynamic framework as described by Talu.¹⁰

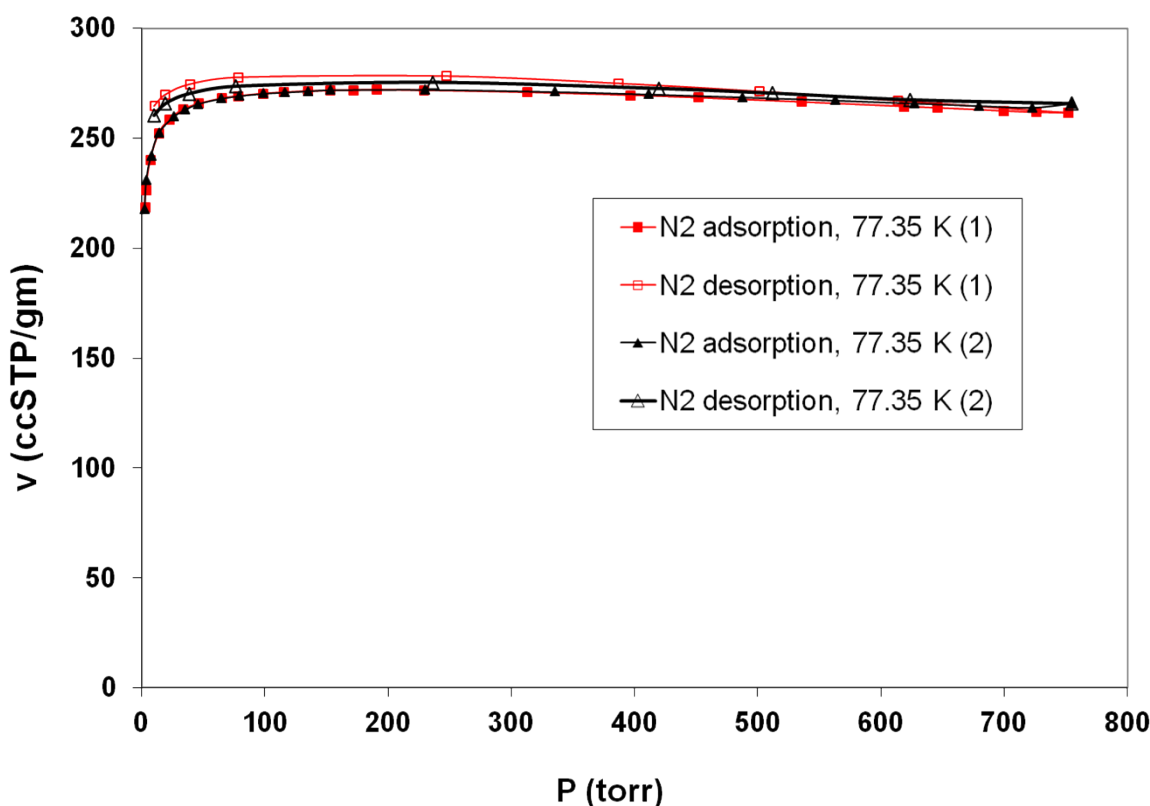


Figure S16. Porosity characterization by nitrogen isotherms at 77.35 K for two samples.

The nitrogen isotherms shown are Type I indicative of micropore adsorption.¹¹ The results for two different samples are in excellent agreement. Hysteresis is not observed within experimental accuracy, as expected from solid structure. The crystal is microporous without any meso- or macro-porosity. The very small upward trend above 700 torr is only indicative of inter-crystal packing porosity. The decreasing trend in isotherm above app. 200 torr can be attributed to the complete filling of the pores although it is within experimental accuracy.

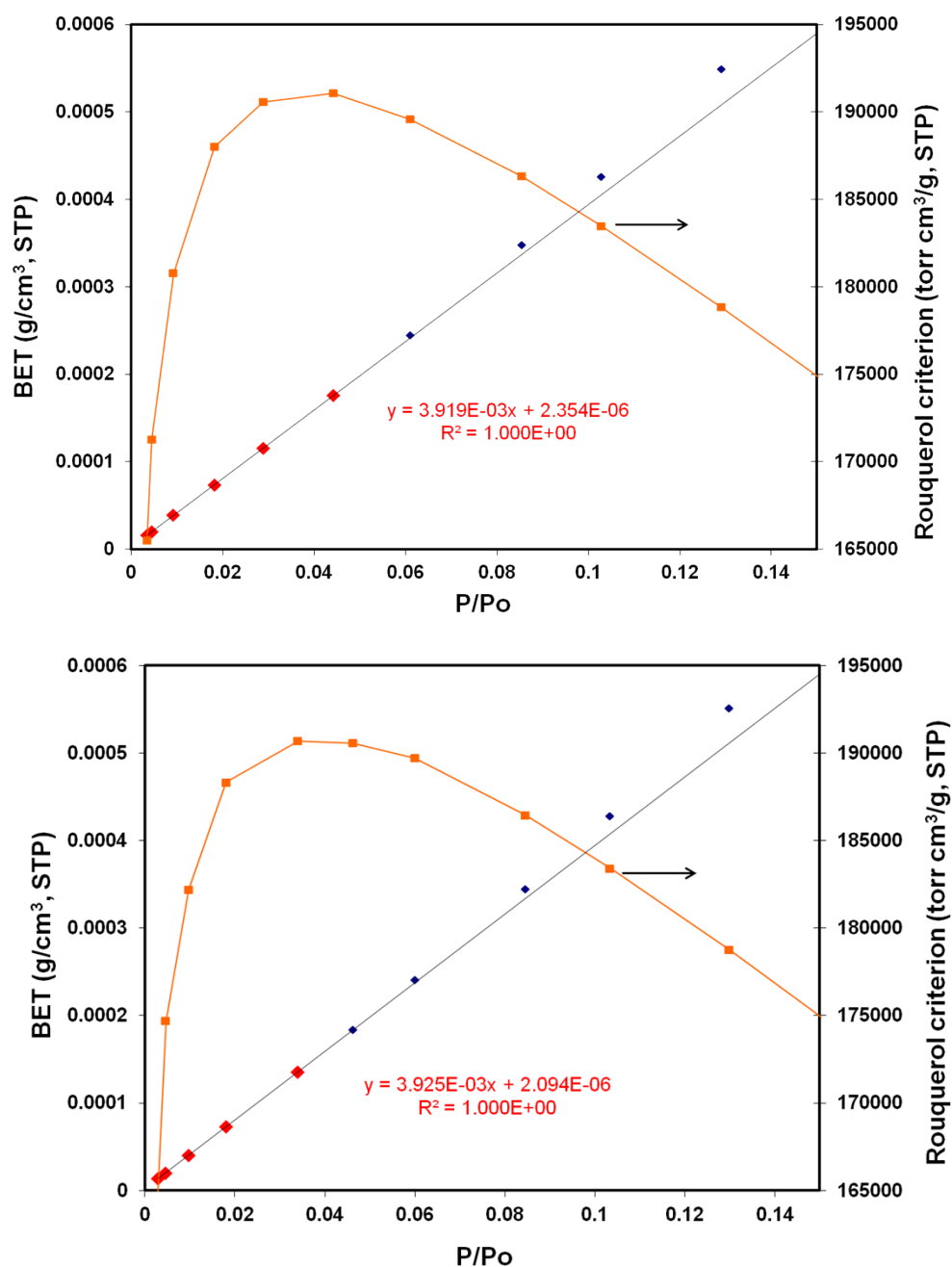


Figure S17. BET plots with Rouquerol criteria for two samples, calculated using nitrogen isotherms. Data points included in calculations were chosen by Roquerol protocol, i.e. $N_{\text{ads}}(1 - P/P_0)$ should be increasing with P/P_0 .¹² At least 5 data points are included in the BET determination for each sample, represented by red diamonds in the figures above.

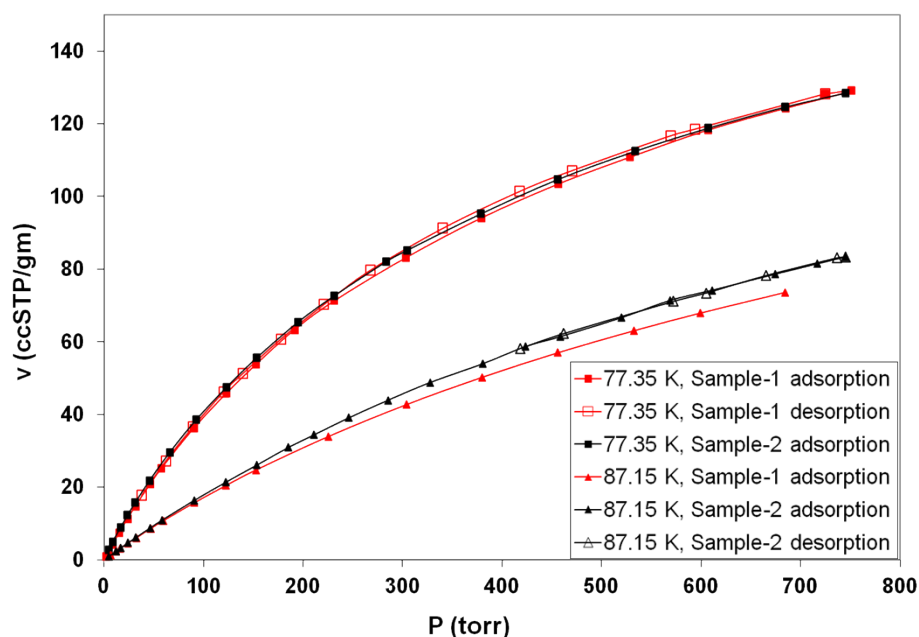


Figure S18: Hydrogen adsorption isotherms of tcpb crystals (two samples). The hydrogen isotherms were measured at two temperatures utilizing liquid nitrogen (77.15 K) and argon (87.35 K) baths.

R = 0.995	Rsqr = 0.990	Adj Rsqr = 0.990			
Standard Error of Estimate = 0.0482					
Analysis of Variance:					
Group	DF	SS	MS	F	P
Regression	2	23.629	11.814	999.999	<0.001
Residual	100	0.233	0.00233		
Variables in Model					
Group	Coef.	Std. Coeff.	Std. Error	F-to-Remove	P
Constant	9.52		0.0851		
1/T	-690.412	-1.039	7.123	9395.54	<0.001
V/T	0.653	0.677	0.0103	3996.202	<0.001
Units: P in torr, V in ccSTP/gm, T in K, Q^{st} in kJ/mol Isotherm Equation: $P = v * \exp(9.52 - 690.412/T + 0.653*v/T)$ Isothermic Heat: $Q^{st} = 8.314/1000*(690.412 - 0.653*v)$					

Table S3: Regression results for Virial isotherm for hydrogen adsorption. To facilitate computation of isosteric heat of adsorption, temperature independent Virial isotherm equation parameters were determined from the isotherms at different temperatures by a single stepwise multilinear regression technique.¹³ The limiting heat of adsorption calculated from regression results is 5.7 kJ/mol. The isosteric heat of adsorption stays constant with amount adsorbed within the experimental accuracy involved in these calculations from isotherms. Terms: DF - degrees of freedom, SS – sum of squares error, MS – mean square error, F – F-statistics, and P – probability.

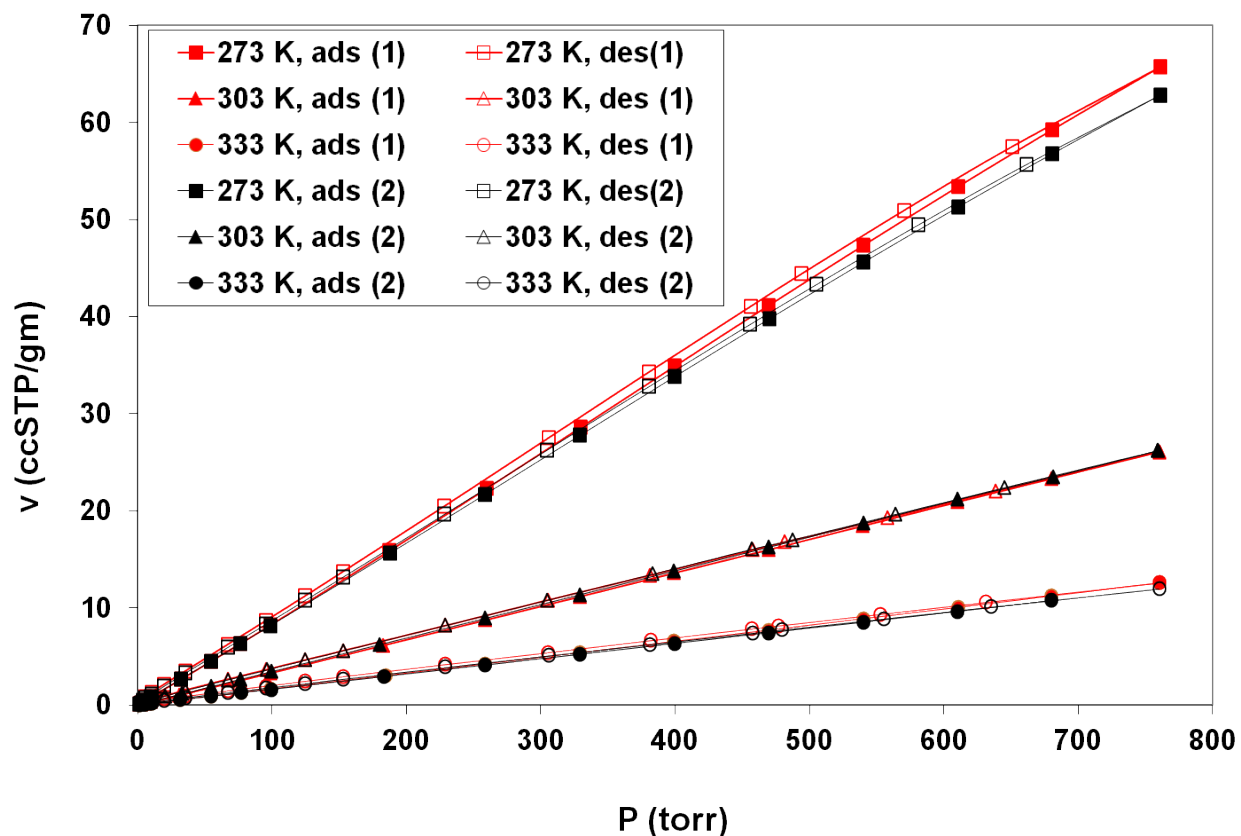


Figure S19: Carbon dioxide isotherms of tcpb crystals (two samples). The carbon dioxide isotherms were measured at 0, 30, and 60°C. No hysteresis is observed since the adsorption/desorption branches are within experimental accuracy of the instruments. The isotherms are linear in the pressure range studied. The limiting isosteric heat of adsorption is estimated to be 22 kJ/mol by an Arrhenius plot of the Henry law constants.

8. References

- [1] H. Furukawa, M. A. Miller and O. M. Yaghi, *J. Mater. Chem.*, 2007, **17**, 3197-3204.
- [2] Apex2 v2011.2-0, Bruker AXS Inc., Madison, WI, USA, 2011
- [3] Saint Plus, V7.68A, Bruker AXS Inc., Madison, WI, USA, 2011.
- [4] G.M. Sheldrick, SADABS, University of Göttingen, Göttingen, Germany, 2008.
- [5] G.M. Sheldrick, SHELXTL v. 6.14, Bruker AXS Inc., Madison, WI, USA, 2008.
- [6] G. M. Sheldrick, *Acta Cryst.*, 2008, **A64**, 112-122.
- [7] G.M. Sheldrick, SHELXL 2014/7, University of Göttingen, Göttingen, Germany, 2014.
- [8] C.B. Hübschle, G.M. Sheldrick and B. Dittrich, *J. Appl. Cryst.*, 2011, **44**, 1281-1284.
- [9] P. van der Sluis and A. L. Spek, *Acta Cryst.*, 1990, **A46**, 194-201.
- [10] S. Gumma and O. Talu, *Langmuir*, 2010, **26**, 17013-17023.
- [11] J. Rouquerol, D. Avnir, C.W. Fairbridge, D.H. Everett, J.H. Haynes, N. Pernicone, J.D.F. Ramsay, K.S.W. Sing and K.K. Unger, *Pure & Appl. Chem.*, 1994, **66**, 1739-1758.
- [12] J. Rouquerol, P. Llewellyn and F. Rouquerol, *Stud. Surf. Sci. Catal.*, 2007, **160**, 49-56.
- [13] O.Talu and R.L. Kabel, *AIChE J.*, 1987, **33**, 510-514.